Chapter 3

Cross-Polarization OCT for In Vivo Diagnostics and Prediction of Bladder Cancer

Elena Kiseleva, Gladkova Natalia, Streltzova Olga, Kirillin Mikhail, Maslennikova Anna, Dudenkova Varvara, Yunusova Katerina and Sergeeva Ekaterina

Additional information is available at the end of the chapter

http://dx.doi.org/10.5772/67473

Abstract

This chapter contains three parts covering recent efforts to increase the accuracy of optical coherence tomography (OCT) differential diagnostics of bladder pathologies. The first part compares the diagnostic efficacy of traditional OCT and cross-polarization OCT (CP OCT); CP OCT and fluorescence cystoscopy (FC) for detecting flat lesions in the bladder at the early stages of cancer. The second part contains a report on achievements in application of CP OCT for detection of recurrent carcinoma in the scar area that is a hardly distinguishable form of bladder cancer using an optimized CP OCT image analysis. The third part of the chapter reviews the results on CP OCT usage for in vivo diagnosis of the bladder cancer after radiation therapy of cervical cancer.

Keywords: cross-polarization optical coherence tomography (CP OCT), bladder cancer, collagen, laser scanning microscopy (LSM), radiation damage

1. Introduction

Bladder cancer can manifest in a variety of different forms, and chronic inflammation plays the key role in its development [1]. One of the origins of bladder cancer development is the side-effect of radiation therapy. The radiation therapy of the uterus or prostate cancer frequently induces substantial alterations in the bladder wall that may progress to bladder cancer. Such side-effects of the radiation therapy of pelvic organs are of particular interest, as they occur in the patients with predicted long life expectancy, and preservation of the life

quality is of comparable importance with recurrence prevention [2]. In this situation, early detection of bladder cancer or pre-cancer manifestations, preferably non-invasive, is the key for timely treatment.

Traditionally, white-light cystoscopy is employed for detection of bladder cancer. Besides the invasiveness and potential risks, white light cystoscopy drawbacks include difficult detection of flat lesions, inaccurate tumor delineation, which leads to complete resection and inability to differentiate between inflammation and malignancy and to determine the tumor grade and stage. In clinical practice, the overcoming of these drawbacks strongly depends on the surgeon's experience [3].

In the last decade, the techniques for diagnosing bladder pathologies were complemented by optical coherence tomography (OCT) being actively introduced into clinical practice [4–6]. OCT is a modern optical non-invasive imaging technique based on the principles of reflectance low-coherence interferometry, which can provide a tissue image to the depths up to several millimeters with spatial resolution down to units of μm. Cross-polarization OCT (CP OCT) is an OCT modality where probing is performed by polarized light; and two conjugated images are being registered in the channels with polarization parallel and orthogonal to initial one (co- and cross-polarization channels, respectively).

Many OCT research groups develop their own approaches for differential diagnostic of early bladder cancer [3, 7, 8]. The combination of OCT diagnostics with image analysis and signal processing (e.g., histograms analysis [9, 10], extraction of optical properties [11], texture analysis [12, 13]) has a high potential for automated differential diagnostics. To bridge the gap between research and clinical use, the potential of CP OCT was systematically investigated for real-time and label-free imaging. Nowadays, the studies are focused on challenging problems such as hardly distinguishable forms of bladder disorders related with cancer. Alterations in normal tissue that occur in the early and late periods after radiation therapy are an actual problem of modern radiation oncology [14] where high potential of the CP OCT was demonstrated.

This chapter contains three parts covering recent efforts to increase the accuracy of OCT differential diagnostics of bladder pathologies. The first part compares the diagnostic efficacy of traditional OCT (equivalent to obtaining co-polarized image only), CP OCT (employing combination of cross-polarized and co-polarized images), and fluorescence cystoscopy (FC) for detecting flat lesions in the bladder at early stages of cancer. In the second part, we report on the recent achievements in application of CP OCT for detection of carcinoma recurrence in scar area using an optimized CP OCT image analysis/quantification platform. The platform is based on detecting alterations in the collagen compartment of interrogated tissue's extra-cellular matrix (ECM). The third part reviews the pilot results of CP OCT employment for in vivo evaluation of the severity of the bladder mucosa damage after radiation therapy of cervical cancer. In addition to morphological analysis with hematoxylin and eosin (H&E) and picrosirius red (PSR) staining, nonlinear laser scanning microscopy (LSM) study was performed to confirm the level of collagen damage and remodeling as a consequence of cancer invasion and radiation therapy.

CP OCT studies of human urinary bladder mucosa during in vivo endoscopic examination described in this chapter were performed with the "OCT 1300-U" system (IAP RAS, Nizhny

http://dx.doi.org/10.5772/67473

Novgorod, Russia). CP OCT device has a forward-looking (en-face) endoscopic probe with outer diameter 2.7 mm that is placed vertically to the mucous surface leaving an imprint on it, so the tissue is taken for histology from the same area and has the same orientation. The CP OCT system is based on superluminiscent diode with central wavelength 1300- and 100-nm bandwidth and has axial resolution ~15 μm and lateral resolution ~25 μm. Using the circular polarized probing light and two signal acquisition channels to detect scattered light that maintained initial polarization and change it to orthogonal one gave an advantage to assess co- ("co-polarized image") and cross-scattering ("cross-polarized image") properties of the tissue up to 1.8 mm in depth. CP OCT image size is 2.5 × 4.0 mm (width × height), image acquisition rate is 0.5 frames per sec. Refer to previous publications [15, 16] for more detailed system descriptions, including the optical phase retardation particulars to enable CP operation.

The fragments of the bladder mucosa from the sites of CP OCT inspection extracted in course of surgery and biopsy were subjects for further histological and LSM examination. Later, CP OCT images were compared to the morphological images. Histologic study included light microscopy with H&E staining and polarized light transmission microscopy with PSR staining for evaluation of structural and spatial organization of collagen fibers; LSM was applied in second harmonic generation (SHG) mode with excitation at the wavelength of 800 nm and spectral detection in the range of 362–415 nm to reveal the distribution of collagen fibers in the bladder mucosa.

The Ethics Committee of Nizhny Novgorod State Medical Academy for scientific research involving human subjects approved the clinical study. All patients voluntarily signed the informed consent for the study.

2. Efficacy of cross-polarization OCT in bladder cancer diagnosis: comparison with traditional OCT, fluorescence cystoscopy, and immunohistochemical study

The early OCT studies of bladder mucosa were performed with traditional time-domain modality equipped with an endoscopic probe. Diagnosis of early bladder cancer was the central topic of OCT studies in urology [4]. After 25 years, the OCT technique significantly improved resulting, in particular in cross-polarization time-domain OCT with common-path optical layout and two signal acquisition channels and in spectral CP OCT modification with the similar characteristics enabling 3D imaging.

2.1. Cross-polarization OCT and traditional OCT at bladder cancer

In course of introduction of CP OCT into clinical practice, the capabilities of this new technique for early bladder cancer detection were assessed in a comparative study with the traditional OCT. To assess the efficacy, the special test was developed. It consisted of two independent stages: assessing diagnostic capabilities of OCT (using a set of co-polarized images) for detecting neoplasia and assessing diagnostic capabilities of CP OCT (using a set of the same clinical cases, but with two images: in co- and in cross-polarization) for the

same task. Statistical evaluation of the diagnostic efficacies of OCT and CP OCT was also performed independently. A total of 116 patients with localized flat suspicious lesions in the bladder were enrolled, 360 CP OCT images were acquired and analyzed. Statistical parameters and general results of the blind recognition tests of CP OCT and OCT images of flat suspicious lesions in the bladder are listed in Ref. [17].

Briefly, it was shown that CP OCT demonstrated higher sensitivity of 93.7% (vs. 81.2%, $p < 0.0001$), specificity 84% (vs. 70.0%, $p < 0.001$), and diagnostic accuracy 85.3% (vs. 71.5%, <0.001) in detecting early malignant changes in flat suspicious zones compared to the traditional OCT technique. The interobserver agreement index *kappa* increased from 0.68 to 0.82 when images in cross-polarization were added. The earlier analysis of more than 500 traditional OCT [4] and CP OCT images of benign and malignant states of the bladder [18] enabled us to formulate visual criteria for assessing CP OCT images in co- and in cross-polarization (**Table 1**).

Higher diagnostic efficacy of CP OCT in detecting early bladder cancer is associated with the ability to detect changes in epithelium and connective tissues. In previous works (see Refs. [17, 19]), it was demonstrated that OCT signal in cross-polarization (**Figure 1a**, upper image) is formed primarily due to cross-scattering from unaltered, well-organized type I collagen. This statement is based on the comparison of the signal level in cross-polarization with the brightness of PSR-stained collagen fiber luminescence in polarized light (**Figure 1j**).

It is known that collagen stained with PSR and examined with polarized light microscopy reveals its birefringent properties, visualized as bright pixels against the background of dark surrounding tissue elements (reference). Collagen type I has red and red-yellow color (thick fibers with thickness ~2–5 μm and higher) and collagen type III—green and green-white color (thin fibers with thickness ~1 μm). Red-orange color of thick-collagen fibers is also associated with densely packed collagen fibers indicative of their maturity [20].

CP OCT image characteristics		**Benign processes in the bladder**	**Malignant processes in the bladder**
In co-polarization:	OCT features	Sharp, high contrast between epithelium and connective tissue in more than 75% of the lateral range of image. The epithelial layer has lower signal level than the connective tissue layer	No or weak contrast between horizontal layers
	OCT type images	Benign	Cancer
In cross-polarization:	OCT features	Uniform signal that may have the structure of horizontal layers	No or weak signal, in some images in the form of isolated spots
	OCT type images	Benign	Cancer

Table 1. Visual criteria for assessing CP OCT images in co- and in cross-polarizations.

http://dx.doi.org/10.5772/67473

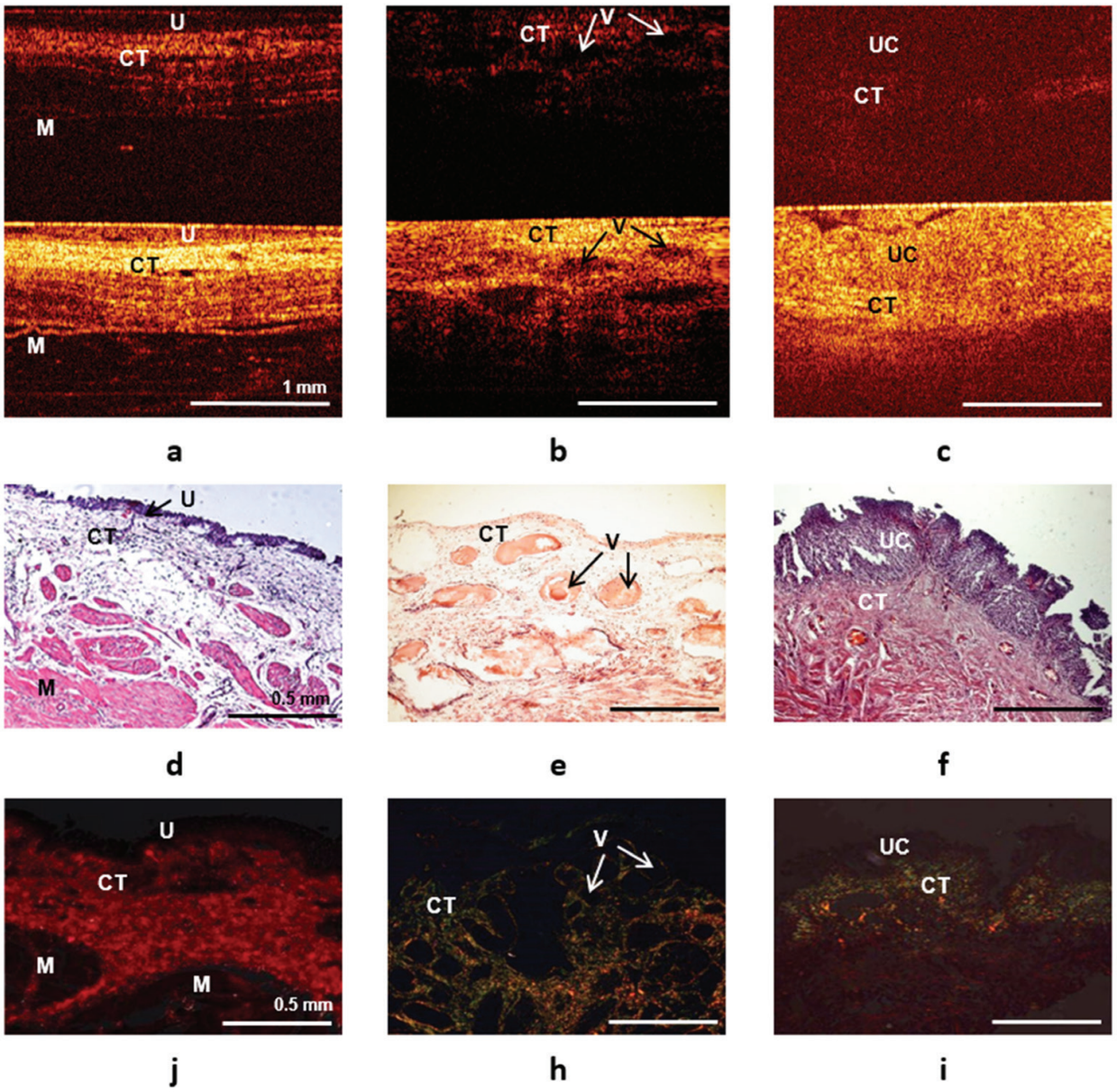

Figure 1. Bladder mucosa in normal state and in pathology. Normal (a, d, j), chronic exudative cystitis (b, e, h) and urothelial carcinoma Ia (c, f, i). CP OCT images (upper panel = cross-polarization, lower panel = co-polarization) (a, b, c), the corresponding histological slides stained with hematoxylin and eosin was used to confirm the diagnosis (d, e, f), stained with picrosirius red and examined with polarized light—to reveal the presence and type of collagen (j, h, i). U—urothelium, CT—connective tissue, M—muscle, V—vessel, UC—urothelial carcinoma.

The loss of collagen polarization properties due to its disorganization at neoplasia (**Figure 1f** and **i**) and massive inflammatory cellular infiltration significantly reduces OCT signal level in cross-polarization (**Figure 1c**, upper image). At the same time, CP OCT images at chronic cystitis in cross-polarization have regions with high-level signal (**Figure 1b**). It is caused by diffuse excessive synthesis and accumulation of collagen fibers (its assembly/bunching in the background of reduced degradation), especially around vessels (sclerosis of vessel wall; **Figure 1e** and **h**).

Based on the qualitative considerations above, it appears that morphological and polarization changes of collagen fibers properties in various pathological states are complex and interrelated.

2.2. Cross-polarization OCT, fluorescence cystoscopy, and immunohistochemical study at bladder cancer

Fluorescence cystoscopy (FC) is one of the techniques to search for regions suspicious for cancer on the inner bladder surface. However, it has low-positive predictive value [21, 22]. Immunohistochemical (IHC) markers for bladder cancer Ta-T2a have potential to improve the diagnostics and help in understanding of carcinogenesis at molecular level [23]. Unfortunately, this technique can be employed only ex vivo. Recent studies of years [19] were aimed to assess the diagnostic accuracy of the combined use of FC and CP OCT with quantitative estimation of OCT signal in cross-polarization for diagnosis of superficial bladder cancer in flat suspicious lesions and analyze epithelial and carcinoma cells proliferation activity by using IHC markers. A total of 26 patients with bladder cancer were enrolled in the study. Total amount of regions of interest was 92; 41 sites with urothelial carcinoma (28 cases of cancer in bladder tissue/13 cases of recurrent cancer in scar tissue) and 51 sites with inflammation (16 mild/35 severe).

The results of the study show that the combined use of FC and CP OCT with quantitative estimation of the OCT signal yields the diagnostic accuracy in detecting bladder cancer in flat suspicious zones of 93.6%, the sensitivity of 96.4%, specificity of 92.1%, positive predictive value of 87%, and negative predictive value of 97.9%, which indicates that the efficacy of this approach is close to that of biopsy.

Since chronic inflammation in the bladder is manifested by the increased proliferative activity of uroteliocytes, IHC study using cell proliferation markers (Ki-67, p53, and p63) allows for more accurate quantification of the urothelium state and the risk of developing urothelial neoplasm. Ki-67, p53, and p63 immunohistochemistry is suggested to be helpful to distinguish dysplastic changes and carcinoma in situ from reactive atypia. These IHC markers were applied for the study of areas where CP OCT images can be classified as cancer type.

The IHC study demonstrated a high level of p53 expression and high proliferation activity (the number of the cells positively stained for Ki-67, p53, and p63 exceeded 50%) in the regions of bladder cancer. Those indices were significantly higher ($p < 0.0001$) comparing to the regions with severe inflammation. In the regions with mild inflammation, the level of Ki-67, p53, and p63 did not differ significantly ($p > 0.05$) from those with severe inflammation [23]. This confirms that the increased urothelium proliferation level in patients with bladder cancer is typical for the entire mucosa and does not depend on the visual manifestations of the inflammatory process [1, 24].

The expression of p63 only in the areas of red fluorescence was significantly higher ($p = 0.038$) than in the areas without fluorescence. The expression of Ki-67 and p53 did not depend on fluorescence.

The study confirms enhanced expression of p53, p63, and Ki-67 in patients with recurrent, highly differentiated superficial (without invasion into the muscular layer) urothelial carcinoma with a low or moderate risk of disease progression [25–28].

Also, a correlation between CP OCT data and IHC markers data was demonstrated. High inverse correlation ($r = -0.732$; $r = -0.647$ and $r = -0.481$, respectively, $p < 0.002$) was demonstrated between the expression of p63, Ki-67, and p53 markers and the CP OCT signal in cross-polarization. The obtained correlations allow suggesting why signal in cross-polarization alters in cases of inflammation and neoplasia. Healthy tissue in co-polarization has a layered structure featuring the epithelium and connective stroma. A neoplastic process characterized by excessive proliferation of urothelial cells losing specificity is accompanied by activation of p53, p63, and Ki-67 expression. On the one hand, active proliferation can change optical properties of epithelial cells; on the other hand, it eventually leads to disorganization of collagen matrix. It was found that the higher the expression of the markers of cellular proliferation and adherence, the more intense loss of cross-scattering properties by connective tissue collagen is registered by CP OCT. However, it is still unclear which process is primary.

3. CP OCT for diagnostics of recurrent bladder cancer

Recurrent forms of bladder cancer are hard to distinguish by routine diagnostic approaches (cystoscopy). In the majority of cases, cancer recurrence at scar is hard to be distinguished from the scar tissue. In this situation, even OCT inspection may fail to provide adequate information due to visual similarity of scar and cancer in a diagnostic OCT image.

To develop an approach to distinguish the recurrence of bladder cancer and the scar, parallel in vivo CP OCT and morphological study of the level of cross scattering and state of collagen was performed for scar tissue (group 1, $n = 30$) and carcinoma in the scar area (group 2, $n = 28$). **Figure 2** shows that sometimes CP OCT images in the scar tissue (a) and in recurrence of carcinoma in scar area (d) look quite similar. In cross-polarization, the OCT signal is heterogeneous: in both cases, there are areas with high, reduced, or absence of signal (**Figure 2a** and **d**, upper images). Analysis of the structural organization of collagen fibers at fiber and tissue levels in the scar tissue (group 1) showed that in condition of chronic inflammation of the bladder mucosa areas of excessive synthesis and accumulation of collagen (see **Figure 2**, red and yellow color on PSR image (b) and intense green color on SGH image (c)) might alternate with not yet formed collagen fibers areas (see **Figure 2**, pale green color or dark areas on PSR image (b) and week or no SHG signal (c)). Analysis of the recurrence of carcinoma on a post-operation scar region (Group 2) revealed that on PSR image areas of carcinoma are dark, and collagen fibers are thin of pale-red color (**Figure 2e**); some of collagen fibers are destroyed. The collagen fibers are loosely stacked and surround cancer cells in SGH image (**Figure 2f**).

OCT image processing and quantification may give an additional valuable information for differentiation these two conditions. A number of previous studies demonstrate that the changes in polarization properties correlate with changes in collagen state [6, 23, 29–31] while

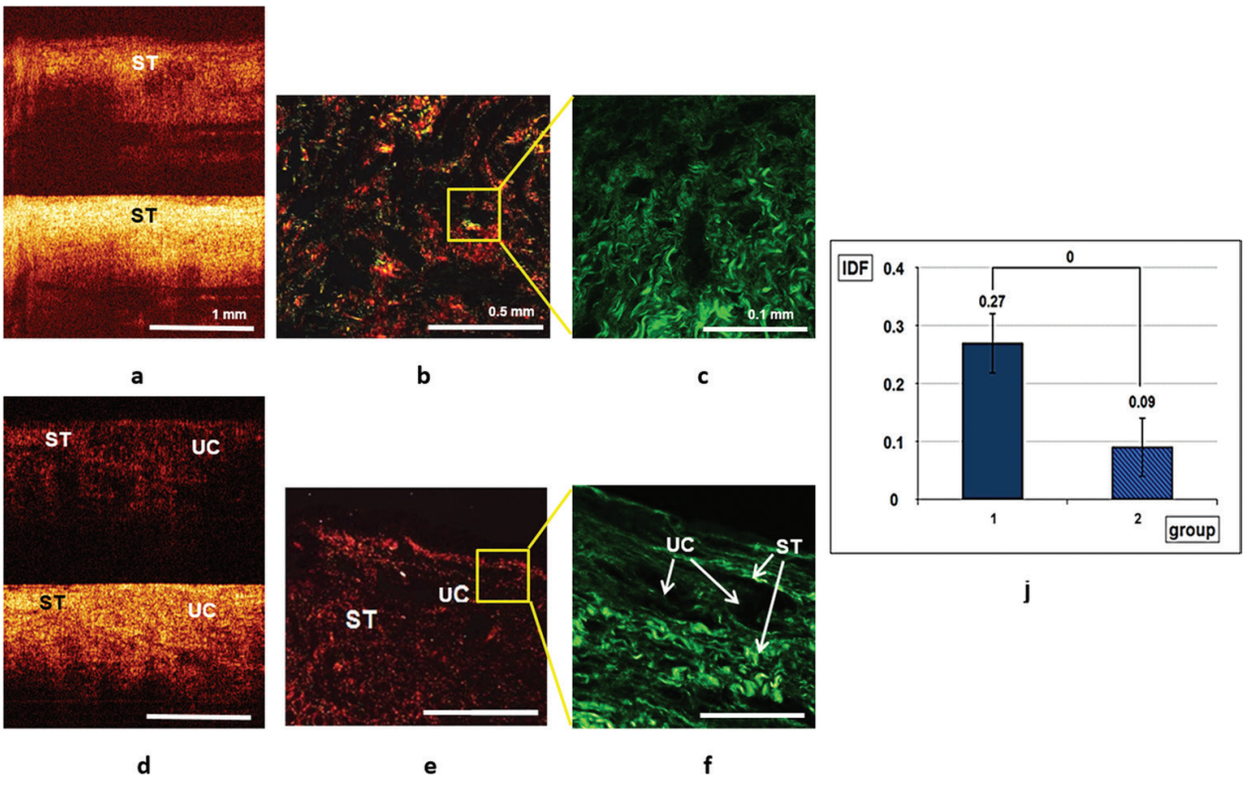

Figure 2. Scar tissue on the bladder mucosa and recurrence of urothelial carcinoma in the scar region. Group 1 (the upper row of images and left column on the diagram), Group 2—recurrence of carcinoma in the scar region (the lower row and left column on the diagram). CP OCT images (upper panel = orthogonal polarization, lower panel = initial polarization) (a, d); corresponding histological slides stained with picrosirius red and examined with polarized light (b, e); SHG images (c, f). ST—scar tissue, UC—urothelial carcinoma.

orientation and the degree of structural organization of collagen at fiber and tissue levels allowed to conclude on the presence of pathology [30]. Quantitative processing of CP OCT images was based on analysis of the cross-scattering properties of the bladder tissue [6]. An integral depolarization factor (IDF) was developed and successfully applied to quantify the collagen state within tissue [31]. IDF is defined as a ratio of the OCT signals in cross-polarization to co-polarization, both averaged over the transverse coordinates.

The results of comparing IDF in the groups of scar tissue (Group 1) and recurrence of urothelial carcinoma in the scar region (Group 2) are presented in **Figure 2j**. A statistically significant difference in IDF values between these two conditions is demonstrated ($p < 0.0001$), which testifies to the possibility of effective cystoscopic recognition of carcinoma in the region of post-operation scar with the IDF/CP OCT platform. It is known that collagen fibers are destroyed under the influence of tumor cell enzymes [32]; this likely decreased the resultant cross-polarization OCT signal. The quantitative assessment of CP OCT images obtained from the suspicious areas of postoperation scars can thus help in distinguishing the appearance of tumor in scar region.

Sensitivity, specificity, and diagnostic accuracy of separating recurrence of carcinoma in region of the bladder scar by quantitative assessment of CP OCT images with IDF are 93, 99, and 97%, respectively.

http://dx.doi.org/10.5772/67473

Intraoperative CP OCT monitoring of completeness of tumor removal was introduced into clinical practice (N.A. Semashko Nizhny Novgorod Regional Hospital) allowing minimizing the number of cancer recurrences at postoperative scar regions.

4. CP OCT for in vivo detection of bladder cancer after radiation therapy

The third paragraph of the chapter reviews the pilot results on CP OCT employment for in vivo detection of the bladder cancer after radiation therapy of cervical cancer.

Bladder cancer that occurs after radiation therapy of malignant neoplasms of the pelvic organs is a special problem in clinical urology. According to European Association of Urology, there is a two- to four-fold increase in the risk of secondary malignant tumors development in the bladder after radiotherapy of tumors of pelvic organs [33]. Recent studies [34, 35] confirmed the increase in the risk of bladder cancer for 1.5–4 times after the course of radiotherapy.

Alterations of normal bladder tissue occurring in the early and late periods after radiotherapy are an unsolved problem in modern radiation oncology [36]. The early side-effects include changes developed in the course of radiotherapy and 100 days after it. Radiation damages that appear after 3 months since radiotherapy procedure are treated as late; sometimes, they may occur in years after irradiation. In addition, in recent years, late effects resulting from long-term persistent severe acute radiation damage called "consequential late effects" are distinguished separately [37]. Specifically, late radiation-induced adverse events are of significant clinical importance [14]. Their severity can vary from clinically insignificant structural abnormalities to severe complications that have a great impact on the quality of patient's life (Cancer Therapy Evaluation Program) [38]. Different classifications including CTCAE, RTOG/EORTC, RILIT, and LENTSOMA were employed to determine the severity of post-radiation damage to normal tissues. Currently, the classification developed by Radiotherapy Oncology Group in collaboration with the European Organization for Research and Treatment of Cancer (RTOG/EORTC, 1995) is the most common classification scale for radiation complications (**Table 2**).

When bladder cancer appears in the irradiated and altered tissues, it becomes extremely difficult to diagnose cancer against edema, hemorrhage, and pronounced changes in the mucosa. Therefore, there is a challenge to differentiate changes induced by ionizing radiation and the changes caused by the tumor growth by standard clinical methods. In this situation, optical diagnostic techniques can play a crucial role in establishing the correct diagnosis.

In our clinical practice during last 2 years, a situation where CP OCT inspection allowed to diagnose bladder cancer in patients previously received radiotherapy for cervical cancer was met twice. Both patients have tumors developed at the background of severe (Grades 3 and 4) late side-effects of radiotherapy (**Table 2**).

Patient T., 65 years old, was hospitalized in urology department for vesico-urinary fistula. In January 2014, she was diagnosed with cervical cancer T3N0M0 (stage III). She received a concurrent chemoradiation therapy (external beam irradiation in a dose of 40 Gy, single dose

Organ tissue	Bladder
Grade 0	None
Grade 1	Slight epithelial atrophy, minor telangiectasia (microscopic hematuria)
Grade 2	Moderate frequency Generalized telangiectasia Intermittent macroscopic hematuria
Grade 3	Severe frequency and dysuria Severe generalized telangiectasia (often with petechiae) Frequent hematuria Reduction in bladder capacity (<150 cc)
Grade 4	Necrosis/contracted bladder (capacity <100 cc) Severe hemorrhagic cystitis
Grade 5	Death directly related to radiation late effects

Table 2. Classification of late radiation bladder damage (RTOG/EORTC, 1995).

2 Gy), brachytherapy in a dose of 25 Gy, single dose 5 Gy). In 18 months after radiation therapy, urine outflow from the vagina and blood in urine appeared. Ultrasound study revealed serozometra and right-side hydronephrosis. Laboratory blood tests showed signs of kidney failure. The right-side nephrostomy under ultrasound control and optical inspection of the bladder was made in November 2015. Cystoscopy revealed an organized blood clot within the bladder cavity. After bladder cavity dilatation, it was found that the bladder bottom was absent resulting in, a fistula defect of 3.5–4.0 cm in diameter. Bullous fabric with disintegration was revealed at the edge of the fistula. Mucosa of the bladder walls was hyperemic and hydropic (**Figure 3a**). Ureteral orifices were not visualized. Therefore, cystoscopy picture was consistent with the picture of Grade 4 radiation bladder damage (fistula, bleeding).

At the same time, bladder mucosa was studied with CP OCT; images of back left and right walls and around the fistula defect were acquired. CP OCT image of the back wall (**Figure 3c**) demonstrates the classic picture of chronic inflammation. Despite contrasted layers in co-polarization and high-level signal from connective tissue fibrosis in cross-polarization, both images feature edema (dark elongated areas, which have vertical shadows) and homogeneous areas originating from inflammatory cell infiltration of the stroma.

CP OCT image of the fistula edge (**Figure 3b**) manifests bullous features: in co-polarization, the image is mostly structureless: only the small area of image in the left has layers of epithelium (the first layer, may be with dysplastic changes), underlying connective tissue (the second layer, brighter) and below the signal abruptly falls (this area is suspicious to cancer); the central and the right side of the image are structureless, indicating neoplasia (**Figure 3b**). In cross-polarization, there is no pronounced signal, which approves the presence of neoplasia, and only small area in left side of the image corresponding to connective tissue demonstrates low-level signal. This flat zone is the suspicious area of the CP OCT image and transurethral biopsy was taken from this site. Morphologically, invasive

http://dx.doi.org/10.5772/67473

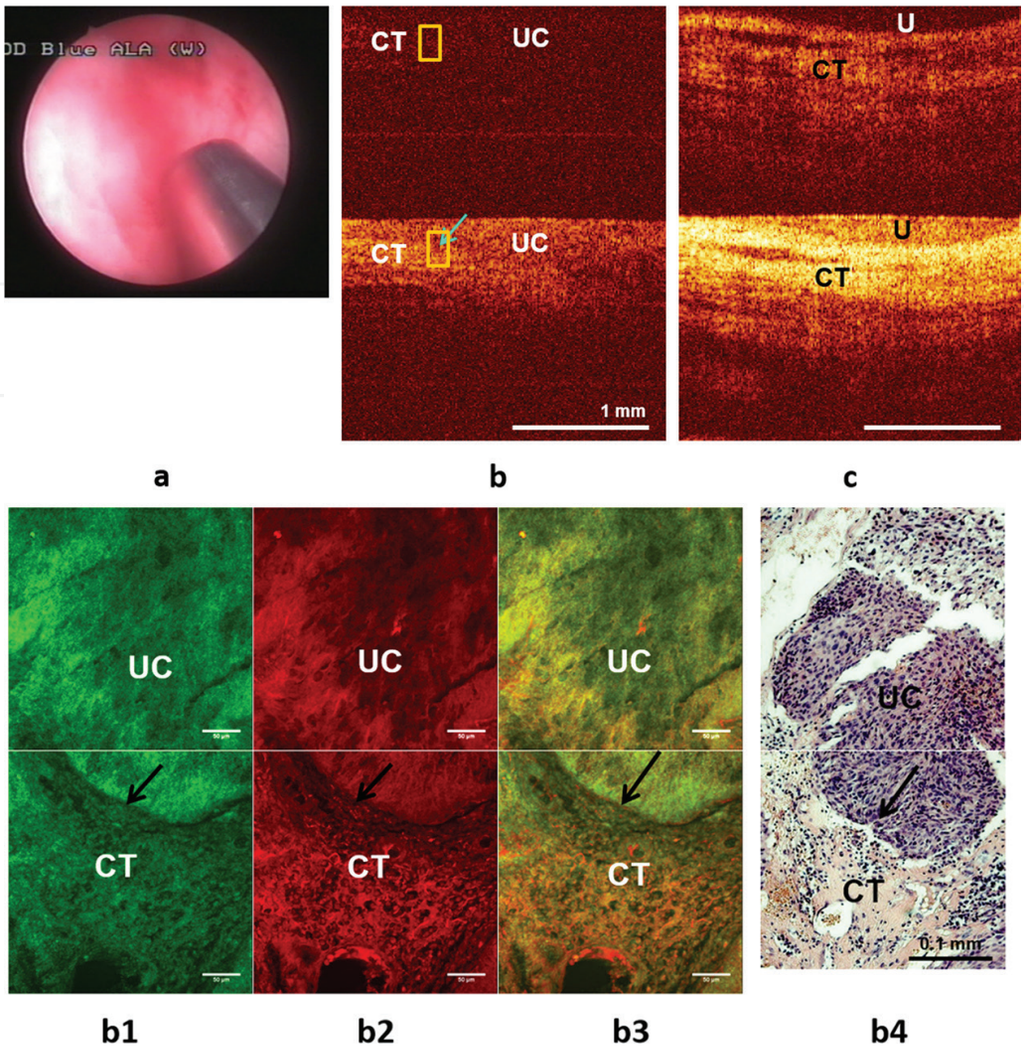

Figure 3. CP OCT guided biopsy of bladder mucosa and LSM study of extracellular matrix in 18 months after the end of radiation therapy. Cystoscopy image of the back wall in a moment of CP OCT study (a), CP OCT images (upper panel = cross-polarization, lower panel = co-polarization): image of tissue suspicious to cancer from border of fistula b), image of benign tissue from the back wall (c), LSM images (SHG (b1), 2PEF (b2) and combined SHG-2PEF (b3)) and histology (H&E) (b4) corresponding to CP OCT image (b). CT—connective tissue; U—urothelium; UC—urothelial carcinoma; arrows indicate border of carcinoma growth; yellow rectangle in (b) indicates area of LSM imaging (b1–b3).

transitional cell carcinoma Grade 2 was diagnosed (**Figure 3b4**). Conglomerates of cancer cells grow into the mucosa and submucosa layers of the bladder wall (area with low signal in co- and dark area in cross-polarization in **Figure 3b**, border of connective tissue is indicated with blue arrow). Carcinoma cells were localized deeper in connective tissue at the one side, whereas at the other side, it starts from the surface. Owing to CP OCT, biopsy was performed and urothelial carcinoma Grade 2 was detected while visually this area looked like inflammation.

We suppose that radiation induced damage of bladder connective tissue induced carcinoma development. In cross-polarization (left side of image), a low level signal from connective tissue is observed, originating from exudative inflammation process. Morphological analysis

revealed congestion, swelling, lymphoid cell infiltrates in mucosa, and, important to mention, degenerative changes in collagen that cause decrease in cross-polarization OCT signal.

In order to determine more accurately the condition of collagen and elastic fibers in connective tissue of mucosa layer multiphoton, microscopy study was conducted. Confocal laser scanning microscope (LSM 710, Carl Zeiss, Germany) was used at the excitation wavelength of 800 nm. Detection was performed simultaneously in two channels by using filters in the wavelength ranges of 362–415 nm and 480–554 nm, with the aim to detect signals indicating SHG emission (green color in the images) and 2PEF emission (red color in the images), respectively. This approach allowed visualization of the collagen (seen in SHG) and primary elastin (seen in 2PEF) fibers in the walls of the bladder within the unstained, dewaxed sections with a thickness of 10 μm.

Two LSM images were combined to demonstrate the boundary between urothelial carcinoma and connective tissue (**Figure 3b1–b3**, the boundary is indicated with black arrow). Numerous small holes in the connective tissue corresponded to inflammatory infiltration, collagen is primary disorganized and looks homogeneous without clearly distinguished fibers (**Figure 3b1**), and elastic fibers are also damaged: they produced weak signal and are presented by fragments in a small amount (**Figure 3b2**). LSM study confirms that the connective tissue of the bladder after radiation therapy of pelvic organs has destructive changes that are preserved for the long time after treatment and in conjunction with chronic inflammation such condition can serve as a background for the cancer development.

Patient N., 41 years old, was urgently hospitalized in urology department with the diagnosis of chronic urinary retention. In 2014, she was diagnosed with cervical cancer T2bN0M0 (stage II), concurrent chemoradiation therapy (external beam irradiation in a dose of 40 Gy, brachytherapy in a dose of 25 Gy, single dose of 5 Gy) was held. In 20 months after the end of chemoradiotherapy, the patient became complaining of difficulty in urinating.

An ultrasound revealed pelvic adhesions, as well as the fact of bladder atony. Trocar cystostomy and cystoscopy study was done. Cystoscopically (**Figure 4a**), the mucous membrane of the bladder was shiny, whitish, trabecular, with tissue granulation on the back wall and in the triangle area; the bladder neck is loose, with a rough surface. Visually, three areas on mucosa were suspicious: in the center of the neck, in the neck close to the right wall, and close to the back wall. The CP OCT study of these areas was conducted, and then three biopsies were taken. Histology revealed presence of urothelial carcinoma Grade 3 complexes in two locations: in the center of the neck and in the neck close to the right wall (**Figure 4b4** and **c4**), where suspicious type of CP OCT images was obtained (**Figure 4b** and **c**). Both images have some features are not common for benign states. They contain structureless low signal areas without clear borders in co- and cross-polarizations at the lower part of the mucosa layer (first layer with a high level signal), and there is no epithelium layer usually manifested by middle intensity signal above the mucosa layer. Moreover, OCT signal from connective tissue in cross-polarization is homogeneous, whereas in norm and inflammation state, an image shows more or less distinct horizontally orientated structures.

http://dx.doi.org/10.5772/67473

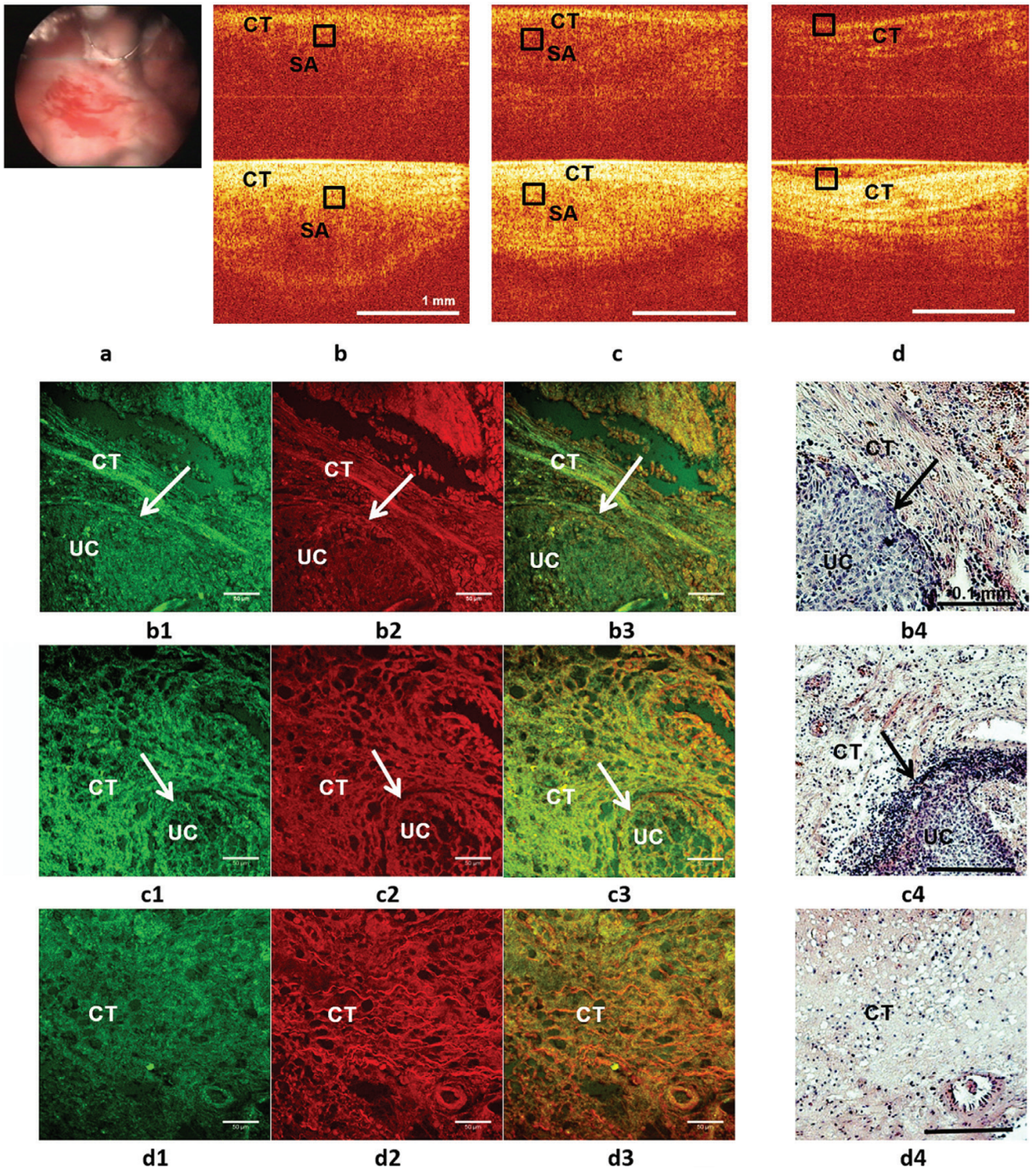

Figure 4. CP OCT of suspicious areas of bladder mucosa and LSM study of extracellular matrix in 20 months after the end of radiation therapy. Cystoscopy image of bladder neck with a loop of resectoscope at the time of biopsy (a), CP OCT images (upper panel = cross-polarization, lower panel = co-polarization): image of suspicious tissue at the bladder neck (b), image of suspicious tissue at the right wall close to the neck (c), image of bening tissue at the back wall (d), LSM images (SHG (b1, c1, d1), 2PEF (b2, c2, d2) and combined SHG-2PEF (b3, c3, d3)) and histology (H&E) (b4, c4, d4) corresponding to CP OCT images (b, c, d). CT—connective tissue; SA—suspicious area; UC—urothelial carcinoma; arrows indicate borders of carcinoma growth; black rectangle in (b, c, d) indicates area of LSM imaging (b1–b3, c1–c3, d1–d3, correspondingly).

CP OCT image of the third visually suspicious area (bladder neck close to the back wall) demonstrates the picture of chronic inflammation (**Figure 4d**) described above. Histology confirms supposed diagnosis: edemas, acute plethora, and round cells infiltration in the mucosa were present (**Figure 4d4**).

LSM images of bladder wall for the patient N. revealed that predominant amount of the fibers produces homogeneous signal similar to the previous case (**Figure 4c1–c3** and **d1–d3**). Only a few individual fibers of collagen and elastin are distinguished. This indicates disorganization processes in extracellular matrix. Loose network and holes in connective tissue in LSM images correspond to morphologically verified inflammation: edema and round a (**Figure 4c4** and **d4**).

Urothelial carcinoma in LSM images looks different: in the bladder neck, collagen in carcinoma is not organized (homogeneous SHG signal, **Figure 4b1**); however, close to the tumor, collagen fibers are straight, densely arranged, and have a prevailing orientation. This may point to aggressive and long-time growth of the carcinoma that starts to produce its own stroma and change the environment around to facilitate the invasion [32, 39]. In the neck close to the right wall, the carcinoma contains no elastic fibers and minimal amount of collagen organized in thin wavy fibers like in surrounding connective tissue, what may indicate infiltrative dissemination of carcinoma cells into loosely packed extracellular matrix **(Figure 4c1–c3**).

The described clinical cases show that extracellular matrix of bladder mucosa after radiation therapy of pelvic organs manifests dystrophic changes that could originate from the side-effects of radiation exposure and subsequent chronic inflammation. Rate of the bladder synchronic cancer in this case is up to 1.5–4 times larger as compared to nonirradiated bladder [34]. We suppose that disorganized collagen and elastic network in mucosa could also promote carcinoma fast growth and facilitate its invasion.

These examples demonstrate that to the patients, who undergone radiation therapy, a special attention and monitoring in the follow-up are required to prevent possible development of radiation induced urothelial carcinoma or detects it as early as possible. In this situation, CP OCT is an excellent minimally invasive tool for bladder mucosa inspection and evaluation of connective tissue state based on data in cross-polarization.

5. Conclusions

This chapter highlighted a novel diagnostic method, CP OCT, with high potential application for bladder pathology diagnosis. CP OCT can be considered an effective complementary in vivo technique to assess flat suspicious lesions in the bladder initially detected by white light or/and fluorescence cystoscopy, whereas the efficacy of these cystoscopy modalities alone or combined with traditional OCT is much lower.

Analysis and quantitative assessment of CP OCT images confirmed the presence of cross-scattering properties of connective tissue stroma in human mucosa that are determined by well-defined spatial and structural organization of collagen matrix. Collagen fibers undergo

significant changes as a result of pathological processes which affect their cross-scattering properties that can be detected and quantified in vivo with CP OCT.

An approach to quantitative, robust, and potentially automated assessment of CP OCT images reflecting the state of bladder collagen fibers was developed. It was shown that IDF can be applied to in vivo detection of clinically relevant pathological states in urology. Differentiating between carcinoma recurrence at post-operation scar and tumor-free scar resulted in diagnostic accuracy of 97%. Thus, CP OCT and IDF quantification have promising potential to visualize and quantify the structural and spatial organization of CF in bladder tissues for clinical disease assessment including differential diagnosis applications.

Acknowledgements

This study was financially supported by the Russian Science Foundation, agreement no. 14-15-00538 (EBK, NDG, VVD) and the grants of the Russian Foundation for Basic Research No. 15-32-20250 (MYuK) and No. 16-07-00655 (OSS, AVM, KEYu).

Author details

Elena Kiseleva[1]*, Gladkova Natalia[1], Streltzova Olga[1], Kirillin Mikhail[2], Maslennikova Anna[1], Dudenkova Varvara[1], Yunusova Katerina[1] and Sergeeva Ekaterina[2]

*Address all correspondence to: kiseleva84@gmail.com

1 Nizhny Novgorod State Medical Academy, Institute of Biomedical Technologies, Nizhny Novgorod, Russia

2 Institute of Applied Physics of the Russian Academy of Sciences, Nizhny Novgorod, Russia

References

[1] Gakis G. The role of inflammation in bladder cancer. Adv Exp Med Biol. 2014;**816**:183-196. DOI: 10.1007/978-3-0348-0837-8_8.

[2] Fiorino C., Valdagni R., Rancati T., Sanguineti, G. Dose-volume effects for normal tissues in external radiotherapy: pelvis. Radiother Oncol. 2009;**93**(2):153-167. DOI: 10.1016/j.radonc.2009.08.004.

[3] Liu J.J., Droller M.J., Liao J.C. New optical imaging technologies for bladder cancer: considerations and perspectives. J Urol. 2012;**188**(2):361-368. DOI: 10.1016/j.juro.2012.03.127.

[4] Zagaynova E., Gladkova N., Shakhova N., Gelikonov G., Gelikonov V., Zagaynova E. Endoscopic OCT with forward-looking probe: clinical studies in urology and gastroenterology. J Biophotonics. 2008;**1**(2):114-128. DOI: 10.1002/jbio.200710017.

[5] Lee C.S., Yoon C.Y., Witjes J.A. The past, present and future of cystoscopy: the fusion of cystoscopy and novel imaging technology. BJU Int. 2008;**102**(9 Pt B):1228-1233. DOI: 10.1111/j.1464-410X.2008.

[6] Kiseleva E.B., Kirillin M.Yu., Feldchtein F.I., Vitkin I.A., Sergeeva E.A., Zagaynova E.V., Streltzova O.S., Shakhov B.E., Gubarkova E.V., Gladkova N.D. Differential diagnosis of human bladder mucosa pathologies in vivo with cross-polarization optical coherence tomography. Biomed Opt Express. 2015;**6**(4):1464-1476. DOI: 10.1364/BOE.6.001464.

[7] Ren H., Yuan Z., Waltzer W., Shroyer K., Pan Y. Enhancing detection of bladder carcinoma in situ by 3-dimensional optical coherence tomography. J Urol. 2010;**184**(4):1499-1506. DOI: 10.1016/j.juro.2010.05.087.

[8] Ikeda M., Matsumoto K., Choi D., Nishi M., Fujita T., Ohbayashi K., Shimizu K., Iwamura M. The impact of real-time 3d imaging by ultra-high speed optical coherence tomography in urothelial carcinoma. BMC Urol. 2013;**13**(65). DOI: 10.1186/1471-2490-13-65.

[9] Kirillin M., Panteleeva O., Yunusova E., Donchenko E., Shakhova N. Criteria for pathology recognition in optical coherence tomography of fallopian tubes. J Biomed Opt. 2012;**17**(8):081413-081421. DOI: 10.1117/1.JBO.17.8.081413.

[10] Yang Y., Wang T., Biswal N.C., Wang X., Sanders M., Brewer M., Zhu Q. Optical scattering coefficient estimated by optical coherence tomography correlates with collagen content in ovarian tissue. J Biomed Opt. 2011;**16**(9):090504. DOI: 10.1117/1.3625247.

[11] Ejofodomi O. Measurement of optical scattering coefficient of the individual layers of the human urinary bladder using optical coherence tomography. ISRN Biomed Imaging. 2014;**2014**. 1-4. DOI: 10.1155/2014/591592.

[12] Kirillin M., Panteleeva O., Agrba P., Pasukhin M., Sergeeva E., Plankina E., Dudenkova V., Gubarkova E., Kiseleva E., Gladkova N., Shakhova N., Vitkin A. Towards advanced OCT clinical applications. In: Lilge L.D., Sroka R., editors. Medical Laser Applications and Laser-Tissue Interactions VII; July 15, 2015; Munich, Germany. Proc. SPIE; 2015. p. 9542. DOI: 10.1117/12.2183794.

[13] Lindenmaier A.A., Conroy L., Farhat G., DaCosta R.S., Flueraru C., Vitkin I.A. Texture analysis of optical coherence tomography speckle for characterizing biological tissues in vivo. Opt Lett. 2013;**38**(8):1280-1282. DOI: 10.1364/OL.38.001280.

[14] Dorr W. Pathogenesis and repair of normal tissue damage. Radiother Oncol. May 2011;**99**(Supp 1):S135. DOI: 10.1016/S0167-8140(11)70460-1.

[15] Gelikonov V.M., Gelikonov G.V. New approach to cross-polarized optical coherence tomography based on orthogonal arbitrarily polarized modes. Laser Phys Lett. 2006;**3**(9):445-451. DOI: 10.1002/lapl.200610030.

[16] Gubarkova E.V., Dudenkova V.V., Feldchtein F.I., Timofeeva L.B., Kiseleva E.B., Kuznetsov S.S., Shakhov B.E., Moiseev A.A., Gelikonov G.V., Vitkin A., Gladkova N.D. Multi-modal optical imaging characterization of athero-sclerotic plaques. J Biophotonics. 2016;**9**(10):1009-1020. DOI 10.1002/jbio.201500223.

[17] Gladkova N.D., Streltsova O.S., Zagaynova E.V., Kiseleva E.B., Gelikonov V.M., Gelikonov G.V., Karabut M.M., Yunusova K.E., Evdokimova O.V. Cross polarization optical coherence tomography for early bladder cancer detection: statistical study. J Biophotonics. 2011;**4**(7–8):519-532. DOI: 10.1002/jbio.201000088.

[18] Gladkova N.D., Zagaynova E.V., Streltsova O.S., Kiseleva E.B., Karabut M.M., Snopova L.B., Yunusova E.E., Tararova E., Gelikonov V.M. Advantages of cross-polarization endoscopic optical coherence tomography in diagnosis of bladder neoplasia. In: Kollias N., Choi B., Zeng H., Malek R.S., Wong B.J.F., Gregory K.W., Tearney G.J., Marcu L., Hirschberg H., Madsen S.J., Mandelis A., Mahadevan-Jansen A., Jansen E.D., editors. Photonic Therapeutics and Diagnostics VI; January 23, 2010; San Francisco, California. Proc SPIE; 2010. p. 754813. DOI: 10.1117/12.841810.

[19] Gladkova N., Kiseleva E., Robakidze N., Balalaeva I., Karabut M., Gubarkova E., Feldchtein F. Evaluation of oral mucosa collagen condition with cross-polarization optical coherence tomography. J Biophotonics. 2013;**6**(4):321-329. DOI: 10.1002/jbio.201200059.

[20] Lattouf R., Younes R., Lutomski D., Naaman N., Godeau G., Senni K., Changotade S. Picrosirius red staining: a useful tool to appraise collagen networks in normal and pathological tissues. J Histochem Cytochem. 2014;**62**(10):751-758. DOI: 10.1369/0022155414545787.

[21] Mowatt G., N'Dow J., Vale L., Nabi G., Boachie C., Cook J.A., Fraser C., Griffiths T.R. Photodynamic diagnosis of bladder cancer compared with white light cystoscopy: systematic review and meta-analysis. Int J Technol Assess Health Care. 2011;**27**:3-10. DOI: 1017/s0266462310001364.

[22] Elferink O.P., Witjes J.A. Blue-light cystoscopy in the evaluation of non-muscle-invasive bladder cancer. Ther Adv Urol. 2014;**6**(1):25-33. DOI: 10.1177/1756287213510590.

[23] Gladkova N., Kiseleva E., Streltsova O., Prodanets N., Snopova L., Karabut M., Gubarkova E., Zagaynova E. Combined use of fluorescence cystoscopy and cross-polarization OCT for diagnosis of bladder cancer and correlation with immunohistochemical markers. J Biophotonics. 2013;**6**(9):687-698. DOI: 10.1002/jbio.201200105.

[24] Acar Ö., Özkurt E., Demir G., Saraç H., Alkan C., Esen T., Somel M., Lack N.A. Determining the origin of synchronous multifocal bladder cancer by exome sequencing. BMC Cancer. 2015;**15**(1):871. DOI: 10.1186/s12885-015-1859-8.

[25] Charfi S., Khabir A., Mnif H., Ellouze S., Mhiri M.N., Boudawara-Sellami T. Immunohistochemical expression of HER2 in urothelial bladder carcinoma and its correlation with p53 and p63 expression. J Microscopy Ultrastruct. 2013;**1**(1–2):17-21. DOI: 10.1016/j.jmau.2013.06.001.

[26] Goebell P.J., Groshen S.G., Schmitz-Drager B.J. p53 immunohistochemistry in bladder cancer—a new approach to an old question. Urol Oncol. 2010;**28**(4):377-388. DOI: 10.1016/j.urolonc.2010.03.021.

[27] Shariat S.F., Bolenz C., Godoy G., Fradet Y., Ashfaq R., Karakiewicz P.I., Isbarn H., Jeldres C., Rigaud J., Sagalowsky A.I., Lotan Y. Predictive value of combined immunohistochemical markers in patients with pT1 urothelial carcinoma at radical cystectomy. J Urol. 2009;**182**(1):78-84. DOI: 10.1016/j.juro.2009.02.125.

[28] Yalçin Ö., Sağlican Y., Özdemir S., Özkan N., Mangir N., Eren F. The Relationship of p16, Ki-67, Bcl-2, P53 and CK20 immune expressions with recurrence in superficial bladder tumors. World J Pathol. 2015;**4**:44-51.

[29] Nadkami S.K., Pierce M.C., Park B.H., de Boer J.F., Whittaker P., Bouma B.E., Bressner J.E., Halpern E., Houser S.L., Tearney G.J. Measurement of collagen and smooth muscle cell content in atherosclerotic plaques using polarization-sensitive optical coherence tomography. J Am Coll Cardiol. 2007;**49**(13):1474-1481. DOI: 10.1016/j.jacc.2006.11.040.

[30] Giattina S.D., Courtney B.K., Herz P.R., Harman M., Shortkroff S., Stamper D.L., Liu B., Fujimoto J.G., Brezinski M.E. Assessment of coronary plaque collagen with polarization sensitive optical coherence tomography (PS-OCT). Int J Cardiol. 2006;**107**(3):400-409. DOI: 10.1016/j.ijcard.2005.11.036.

[31] Gubarkova E.V., Kirillin M.Y., Sergeeva E.A., Kiseleva E.B., Snopova L.B., Prodanets N.N., Sharabrin E.G., Shakhov E.B., Nemirova S.V., Gladkova N.D. Cross-polarization optical coherence tomography in evaluation of atherosclerotic plaque structure. Sovrem Tehnol Med. 2013;**5**(4):45-54. DOI: 10.17691/stm2015.7.4.05.

[32] Provenzano P.P., Eliceiri K.W., Campbell J.M., Inman D.R., White J.G., Keely P.J. Collagen reorganization at the tumor-stromal interface facilitates local invasion. BMC Med. 2006;**4**:38. DOI: 10.1186/1741-7015-4-38.

[33] Chrouser K., Leibovich B., Bergstralh E., Zincke H., Blute M. Bladder cancer risk following primary and adjuvant external beam radiation for prostate cancer. J Urol. 2008;**159**(5 Suppl):S7-S11. DOI: 10.1016/j.juro.2008.03.131.

[34] Jacobs B.L., Lee C.T., Montie J.E. Bladder cancer in 2010: how far have we come?. CA Cancer J Clin. 2010;**60**(4):244-272. DOI: 10.3322/caac.20077.

[35] Suriano F, Altobelli E, Sergi F, Buscarini M. Bladder cancer after radiotherapy for prostate cancer. Rev Urol. 2013;**15**(3):108-112.

[36] Dorr W. Radiation effect in normal tissue—principles of damage and protection. Nuklearmedizin. 2010;**49**(1):S53-S58.

[37] Hendry J.H., Jeremic B., Zubizarreta E.H. Normal tissue complications after radiation therapy. Rev Panam Salud Publica. 2006;**20**(2–3):151-160. https://dx.doi.org/10.1590/S1020-49892006000800012.

[38] Cancer Therapy Evaluation Program. Common Terminology Criteria for Adverse Events (CTCAE) v4.0 [Internet]. 2010. [Updated: 2016.08.07]. Available from: https://ctep.cancer.gov/protocoldevelopment/electronic_applications/ctc.htm#ctc_40 [Accessed: 2016.08.10].

[39] Thrasivoulou C., Virich G., Krenacs T., Korom I., Becker D.L. Optical delineation of human malignant melanoma using second harmonic imaging of collagen. Biomed Opt Express. 2011;**2**(5):1282-1295. DOI: 10.1364/BOE.2.001282.

IntechOpen

IntechOpen